Assessment of Converter Sludge from Esfahan Steel Company as a Persulfate Nano-Activator for Permeable Reactive Barriers (Prbs) in Landfill Leachate Treatment

Soubh, A.M., Abdoli, M. A.,* Baghdadi, M., and Aminzadeh, B.

Graduate Faculty of Environment, University of Tehran, P.O.Box 1417853111, Tehran, Iran

ABSTRACT: The present research studies the performance of Converter Sludge (CL) as a nano-activator of persulfate (PS) in Permeable Reactive Barrier (PRB) as an in-situ technology for leachate treatment. In batch experiments, the acidic conditions (pH = 3) have been the most suitable for removal operations, where COD and NH_3 removal efficiencies are 69.15% and 60.96%, respectively. The Box–Behnken design (BBD) has been employed to optimize three parameters, namely PS/ COD ratio, CS dose, and pore volume (PV), using COD and NH_3 of leachate landfill as the target pollutant. The BBD is considered a satisfactory model to optimize the process. Under optimal conditions (PS/COD ratio: 3.47, CS dose: 3.09 g L^{-1}, and PV: 4.27), the measured values of the COD and NH_3 removal efficiencies have been 74.2 and 66.8, respectively, all within the 95%- prediction intervals, which indicate the model's success in predicting removal values. The biodegradability (BOD_5/COD) of the real leachate has been enhanced from 0.25 to 0.77, with the toxicity of real leachate getting decreased by more than 90%.

Keywords: COD, NH_3, Removal, Box–Behnken design, BOD_5/COD, Toxicity.

INTRODUCTION

Landfill leachate is a high concentrated sewage, consisted of the decomposition of substances in the waste (Chou et al., 2013; Mokhtarani et al., 2016). Accordingly, the lagoon leachate of Tehran's municipal waste disposal site mainly contains very high organic loads, being characterized by a high percentage (68.8%) of biodegradable materials and moisture, which pose a serious threat to surface water and groundwater (Pazoki et al., 2014; Soubh & Mokhtarani, 2016). Considering that most regions of Iran are in dry and semi-arid regions (73%) and that the country suffers from a lack of rainfall and water resources,

proper management of the landfill leachate is a very big challenge (Madani et al., 2016; Pazoki et al., 2014; Soubh & Mokhtarani, 2016). Tehran's landfill leachate contains a massive load of pollutants, which makes treatment a real problem; as a result, biological treatment is not sufficient for this purpose and it often needs post-treatment (Pazoki et al., 2014; Soubh & Mokhtarani, 2016). Recycling leachate via re-pumping it to the landfill or discharging it to domestic sewage are low cost methods, yet definite specifications must be achieved prior to that (Abbas et al., 2009; Renou et al., 2008; Van-Nooten., 2010).

With Persulfate (PS) ($S_2O_8^{2-}$) belongs to peroxygen family, having a strong redox potential (E^o= 2.01 V), which leads to its

---

* Corresponding Author, Email: mabdoli@ut.ac.ir

wide use in minimization of the pollutants (Abu Amr et al., 2013; Zhen et al., 2012). When activated with activators like heat, transition metal ions, UV radiation, ozone, etc., it can give better results in terms of generating sulfate radical (SR) with redox potential ($SO_4^{\bullet-}$, E^o= 2.4 V) in sulfate radical-based advanced oxidation processes (SR-AOPs) (Abu Amr et al., 2013; Cao et al, 2008; Deng & Ezyske, 2011; Lin et al, 2011). Recently, it has been widely used to refine landfill leachate (Chou et al., 2013; Hilles et al, 2016; Soubh & Mokhtarani, 2016) and its use has also yielded satisfactory results when used in Permeable reactive barrier (PRB) technology (Al-Shamsi & Thomson, 2013). In recent years, this technique has been used to remediate MSW landfill leachate whose performance has improved by adding materials to PRB that degrade target pollutants by improving chemical reactions with reactive media (Chiemchaisri et al, 2015). Different materials have been used in PRB media such zero-valent iron (ZVI) (Bartzas et al, 2006), fly ash zeolites (Czurda & Haus, 2002), and zeolite-sand mixtures (Joanna & Kazimierz, 2013). Wide slice of materials such as atomized slag material (Chung et al, 2007), ZVI and mixture of ZVI with zeolites (Ju et al, 2009), industrial by-products (Bhalla et al., 2014), ferric chloride sludge and vegetation-containing sand (Chiemchaisri et al., 2015), and natural Red Earth with Peat (Abhayawardana, 2015) have been applied for the treatment of contaminants from landfills in PRB, successfully employed for removal of both ammonium (NH_4) and chemical oxygen demand (COD) from Landfill Leachate (Liu et al., 2011; Van-Nooten et al., 2010). However, this technique is usually designed for treatment of dissolved plume, not the source zone, itself (Al-Shamsi & Thomson, 2013). The basic limitation of this technique is its costliness, e.g., costs of soil drilling, transport, and pumping and treat technique

(Huling & Pivetz, 2006; NRC, 1999; Siegrist et al., 2011). Yet, it can be reduced to less than 50%, if the latter is dispensed (Bhalla et al., 2014).

Increased quantities of industrial waste can pose a serious risk to the environment in case they are not disposed properly. Reusing waste in various fields can be considered an effective method. For example, in the agricultural sector, steel industry waste is utilized to improve the soil (Karimian et al., 2012). On the other hand, fly ash, bottom ash, and converter slag are being used to treat sewage and landfill leachate (Oh et al., 2007; Ortiz et al., 2001). Each year, hundred tons of iron industry waste, such as converter sludge (CS), are being produced from Esfahan Steel Company of Iran (Bozkurt et al., 2006; Karchegani et al., 2014). Thanks to its rich iron oxides, it can be considered a good source of iron, which is a catalyst of PS (Diao et al., 2016; Karimian et al., 2012; Romero et al., 2010).

The present search employs the wastes from iron industries in integrated landfill leachate management. Fig. 1 shows the schematic overview of two scenarios for the beneficial use of CS as activator of PS in PRB technology. In the first scenario, the nanoparticles have been injected into the source zone for treatment of leachate plume. In the second, this technique can also be used for treatment of the collected leachate landfill. The tests in this study have been conducted on real collected leachate.

MATERIALS AND METHODS
The converter sludge (CS) was first gathered from Esfahan Steel Company, Iran, next to be ground and sieved through a 60 mesh sieve. All chemicals, employed for the analysis, were of analytical grade and were obtained from reliable companies. The test kits for determination of COD and NH3 were purchased from HACH Company (U.S., Loveland,
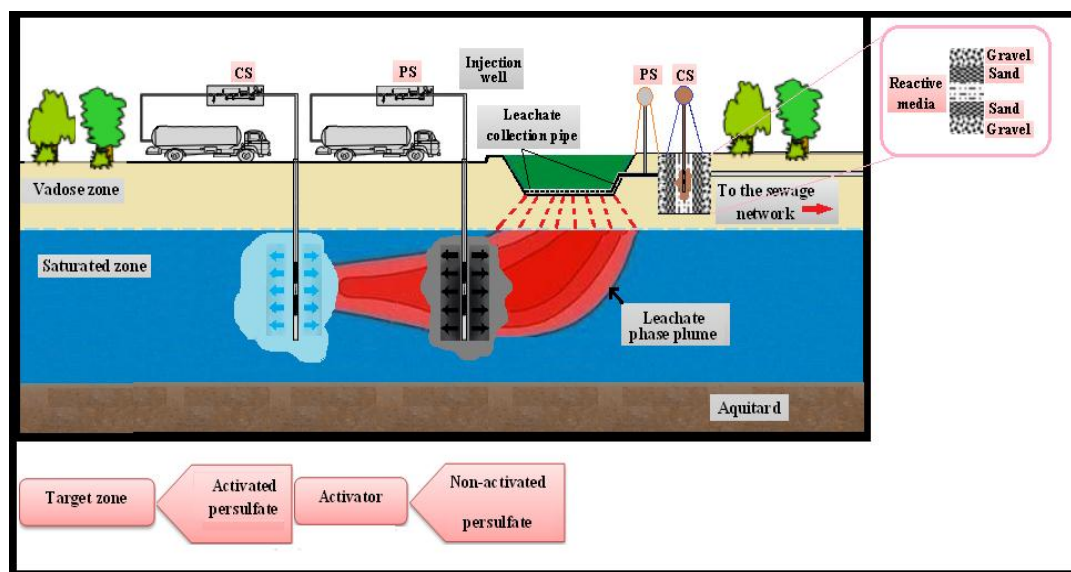
Fig. 1. Schematic overview of beneficial in-situ use of CS with PS for treatment of a source zone

Colorado), with deionized water being used during the experiments. Fresh leachate was brought from Aradkouh's landfill, located in Tehran, Iran, which accommodates 8000 tons solid waste per day (Pazoki et al., 2014). Table 1 shows the characteristics of raw leachate. The fresh leachate transferred to the laboratory was kept in refrigerator at 4 °C so that any change, likely to happen up until the experiments, could be diminished (Soubh & Mokhtarani, 2016).

Laboratory experiments were designed to simulate conceptual model (Fig. 2). The permeability barrier simulator reactor, used in this study, was a circular column made of Plexiglass, 50 cm high with an internal diameter 4.4 cm, containing 15 cm sand in upper and lower sections along with as much as 5 cm of the reactive bed of mixture (sand + CS) in between. Both sides of column were covered with 3 cm of gravels with granulation (2-2.38mm) to retain the aquifer material in the column. Stainless steel mesh was used for optimal flow distribution. The leachate, loaded with non-activated PS, was passed through from the activation zone, which contained CS. Un-polluted sand was prepared by Waseem

Daoud method. Firstly, sand was soaked for 24 hours and then got washed up (100-mesh). After that, it remained in a temperature of 105° C to dry (Daoud et al., 2015). The granulation of the sand, used in this research, ranged between 0.595 and 1.19 mm. Peristaltic pump was used to provide a constant flow rate of 4 ml/min (bottom-up) for all experiments.

Table 1. Characteristics of the used leachate

Parameter	Average*	Unit
pH	6.3	—
COD	20000	mg L^{-1}
NH$_3$	1250	mg L^{-1}
BOD$_5$	4950	mg L^{-1}
TDS	3250	mg L^{-1}
EC	18.2	mS cm^{-1}

* Number of replicates: 3

The surface morphology was investigated, using SEM analysis (VEGA//TESCAN -Czech). EDS (Rontec- Germany) analysis was also used in order to examine the surface elemental composition of CS, with X-ray diffraction (XRD) patterns of converter sludge and slag being acquired, using an X-ray diffractometer (X'Pert PRO MPD, PANalytical Company) with a CuKa radiation source of 40 kV and 40 mA.
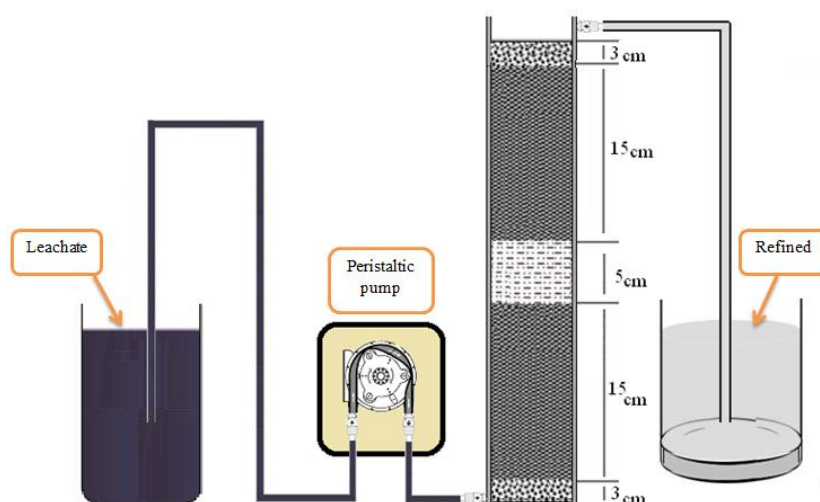
Fig. 2. Schematic laboratory setup

COD and NH$_3$ concentrations were determined, using a spectrophotometer (HACH, DR 5000). PS interference in the COD was taken into consideration by means of Soubh et al.'s method (2018). BOD$_5$ was determined by a BOD measurement system (OxDirect), and a Metrohm 691 pH-meter was employed to measure the potential hydrogens in the solutions. Electrical Conductivity (EC) and Total Dissolved Solids (TDS) were measured with a multi-meter, equippedwith a conductivity electrode (WTW COND 7110, inoLab). A GS-6890N Agilent gas chromatograph, coupled with an MS-5973N Agilent mass spectrometer, was used to identify the intermediate products in raw and treated leachate. The GC-MS, applied for this purpose was equipped with a capillary column (TRB-S), 60 m long, 0.5 μm thick, and 320 μm in internal diameter. The initial temperature of the column was set to 40 ℃ for 5 min. Afterwards, it was increased to 280 ℃ at a rate of 10 ℃ per min. Inlet and AUX temperature were 250 and 280 ℃, respectively. One microliter of the sample was injected into the GS column (its split ratio being 1:1).

The leachate toxicity was assessed, using Eq. 1 (Soubh & Mokhtarani, 2016). In this context, components of fish LC$_{50}$ were initially appraised via TEST (Toxicity Estimation Software Tool) software and classified, according to Table 2 into five main categories, which corresponded to proportions X, A, B, C, and D of leachate components (Ranjbari & Mokhtarani, 2018).

$$\text{Toxicity}(\%) = \sum X(\%) \rightarrow \sum \frac{A\%}{10} + \sum \frac{B\%}{100} + \sum \frac{C\%}{1000} + \sum \frac{D\%}{10000} \tag{1}$$

Table 2. Chemical waste toxicity categories

Toxic category	Fish LC$_{50}$ (ppm)
X	<0.01
A	0.01–<0.1
B	0.1–<1.0
C	1.0–<10.0
D	10.0–100.0

At batch process, the removal efficiency of COD and NH$_3$ were conducted at different pH rates (i.e., 3, 5, 7, and 9) with PS/COD mass ratio of 2, CS dose of 1.5 g L^{-1}, and 60 min of reaction time, where the appropriate pH was chosen.

At continuous processes, The RSM was utilized to estimate the relation as well as interactive effects of discrete parameters PS/COD ratio, activator dose (CS), and Pore volume (PV) on COD and NH$_3$ removal. In this context, the Box-Behnken Design (BBD), which is a second-order polynomial model (Eq. 2) was employed to

398

determine the optimal conditions for critical factors. Where R is the predicted response for removal efficiency; β_0, the intercept parameter; β_i, β_{ii}, and β_{ij}; parameters for linear, quadratic, and interaction factor effects; x_i and x_j, independent variables; and ε, the error. The analysis of the variance (ANOVA) was used to determine the homogeneity between the model and the empirical results, with F-test being applied to verify whether the model could predict a significant variation in the experimental data or not. The probability p value was used to estimate whether F was large enough to indicate any statistical significance (Kumar et al., 2008). The model was developed, using a software program called Design Expert v.10.0.3. The levels of the selected variables (low, center, and high) were given the values of -1, 0, and 1, respectively, as can be seen in Table 3. Finally, the BOD₅/COD as well as

toxicity of raw and treated landfill leachate was examined under optimal conditions.

$$R = B_0 + \sum_{i=1}^{k} B_i X_i + \sum_{i=1}^{k} B_{ii} X_i^2 + \sum_{i=1}^{k} \sum_{j=i+1}^{k} B_{ij} X_i X_j + \varepsilon \qquad (2)$$

The empirical results were achieved under selected conditions of BBD to be used in statistical operations. They can be seen in Table 4. Total empirical design was carried out, using 17 tests with five iterations at the center and removal efficiencies were calculated according to Eq. 3, below:

$$Removel \ (\%) = \left[\left(C_i - C_f \right) / C_f \right] \times 100 \qquad (3)$$

where C_i and C_f stand for initial and final concentrations of COD and NH₃, respectively.

Table 3. The levels of experimental factors for full factorial design

Factors	Symbols	Range and levels		
		(−1)	0	(+1)
PS/ COD ratio	A	1	2.5	4
CS dose (g L⁻¹)	B	1	2.5	4
PV (ml)	C	1	6.5	12

Table 4. The BBD design matrix and empirical results

Run	Factors			Removal efficiency (%)			
	PS/COD ratio A	CS dose (g L⁻¹) B	PV C	COD		NH₃	
				Actual	Predicted	Actual	Predicted
1	2.5	2.5	6.5	61.60	60.74	52.90	50.86
2	2.5	1	1	49.90	51.64	41.60	43.25
3	1	2.5	12	24.80	25.86	13.80	14.56
4	4	1	6.5	43.60	42.93	32.20	31.31
5	4	4	6.5	72.80	73.55	61.90	63.74
6	2.5	2.5	6.5	60.10	60.74	50.90	50.86
7	2.5	2.5	6.5	62.90	60.74	50.40	50.86
8	1	2.5	1	39.80	38.81	30.50	30.69
9	4	2.5	1	73.20	72.14	62.90	62.14
10	4	2.5	12	44.10	45.09	33.90	33.71
11	2.5	2.5	6.5	58.20	60.74	50.30	50.86
12	2.5	1	12	29.20	28.89	11.90	12.97
13	1	1	6.5	24.50	23.75	14.80	12.96
14	2.5	4	12	56.90	55.16	48.10	46.45
15	2.5	2.5	6.5	60.90	60.74	49.80	50.86
16	1	4	6.5	39.50	40.18	30.60	31.49
17	2.5	4	1	72.10	72.41	61.80	60.73

RESULTS AND DISCUSSION

Fig. 3 illustrates the XRD pattern of CS, showing that it appeared abundantly in iron oxides, making it more likely to be used as a source of iron ions. SEM images of CS can be seen in Fig. 4 (A and B). Accordingly, the largest particle size of CS was within range (200-800 nm). It can increase the contact area between Cs and PS. Table 5 demonstrates EDS analysis of the atomic percentage of C, O, Si, Ca, Mn, and Fe, present in CS powder, showing a high percentage (70%) iron.
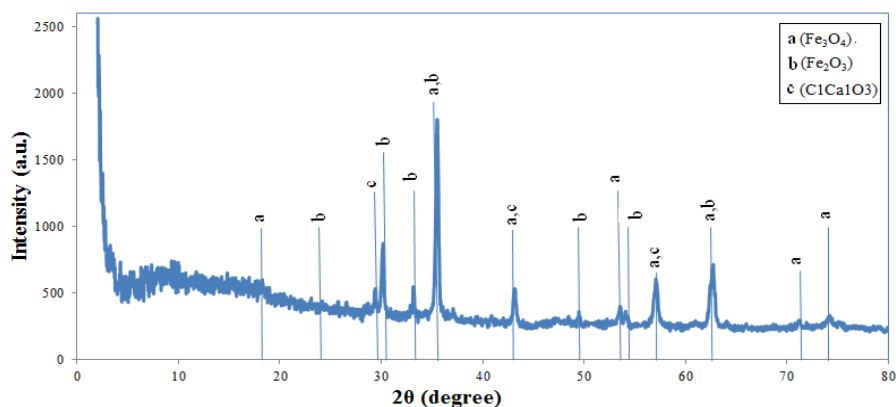
Fig. 3. Powder XRD pattern of converter sludge (CS)
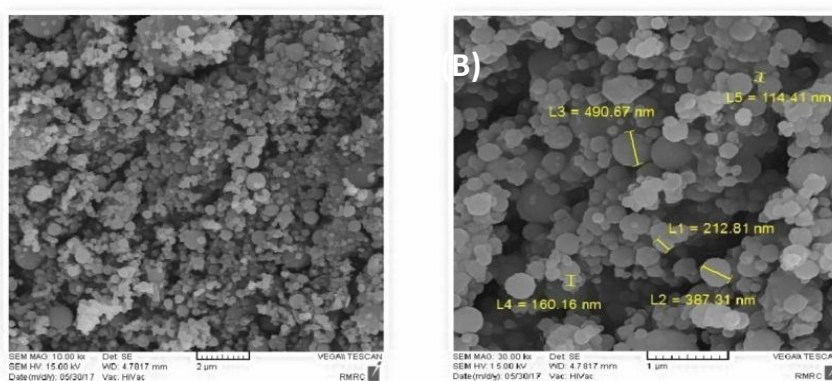
Fig. 4. SEM images of converter sludge at (A) 10 KX and (B) 30 KX

Table 5. EDS Analysis of CS

Element	W/W%
C	0.011
O	19.95
Si	0.54
Ca	3.5
Mn	3.97
Fe	72.03

The pH is considered an important and influential factor on sulfate radical generation (Liang et al., 2007; Shiying et al., 2009); therefore, the experiments aimed at removing COD and NH$_3$ with different pH values (3, 5, 7, and 9). As shown in Fig. 5, the acidic conditions were the best candidate for so doing. They led to maximum removal efficiency of COD (69.1%) and NH$_3$ (60.9%) at a pH rate of 3.0. The reason for this was that iron oxides got released from ferrous and ferric irons, in accordance to both Eq. 4 and Eq. 5. The ferrous and ferric irons can activate persulfate, too, based on Eq. 6 and Eq. 7 (Devi et al., 2010; Fang et al., 2013; Hou et al., 2012; Liang et al., 2004; Liu et al., 2013; Nachiappan & Gopinath, 2015; Virtanen et al., 1997; Yan et al., 2011).
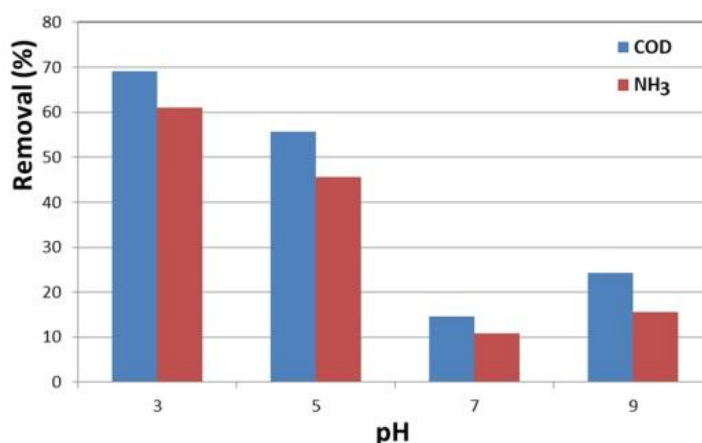
Fig. 5. Influence of pH on COD and NH₃ removal (PS/COD ratio of 2; CS dose of 1.5 g/L; reaction time of 60 min)

$$Fe_3O_4 + 8H^+ \rightarrow 2Fe^{3+} + Fe^{2+} + 4H_2O \qquad (4)$$

$$Fe_2O_3 + 6H^+ \rightarrow 2Fe^{3+} + 3H_2O \qquad (5)$$

$$S_2O_8^{2-} + Fe^{3+} \rightarrow 2SO_4^{\bullet-} + Fe^{2+} \qquad (6)$$

$$S_2O_8^{2-} + Fe^{2+} \rightarrow SO_4^{\bullet-} + SO_4^{2-} + Fe^{3+} \qquad (7)$$
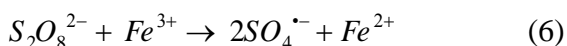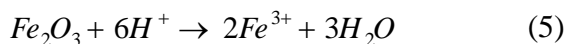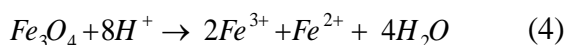
Furthermore, highly acidic conditions may also cause further breakdown of persulfate into sulfate free radicals, according to Eq. 8 and Eq. 9 (Ahmad et al., 2015; Huling et al., 2011).

$$S_2O_8^{2-} + H^+ \rightarrow HS_2O_8^- \qquad (8)$$

$$HS_2O_8^- \rightarrow H^+ + SO_4^{2-} + SO_4^{\bullet-} \qquad (9)$$
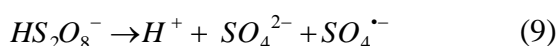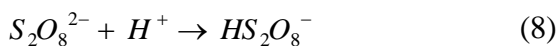
As can be seen in Fig. 5, by further increasing pH, a significant decrease occurred in removal efficiency, which can be attributed to formation of less reactive iron complexes under weak acidic conditions ($5 < pH < 7$) in accordance to Eq. 10 to Eq. 13. Finally, ferric ions can precipitate as iron hydroxide, subsequently lowering the activation rate. (Govindan et al., 2014).

$$Fe^{+2} + H_2O \rightarrow FeOH^+ + H^+ \qquad (10)$$

$$Fe^{+3} + H_2O \rightarrow Fe(OH)^{2+} + H^+ \qquad (11)$$

$$Fe^{+3} + 2H_2O \rightarrow Fe(OH)_2^+ + 2H^+ \qquad (12)$$

$$2Fe^{+3} + 2H_2O \rightarrow Fe_2(OH)_2^{4+} + 2H^+ \qquad (13)$$
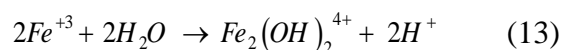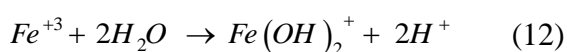
By increasing the pH to 7, production of sulfate radical was entirely stopped. The removal efficiencies were 14.6% and 10.8% for COD and NH₃, respectively. Based on Eq. 14, PS anions, under such conditions, often hydrolyze to hydrogen peroxide (House., 1962; Kolthoff & Miller, 1951; Liang & Guo, 2012).

$$S_2O_8^{2-} + 2H_2O \rightarrow 2HSO_4^- + H_2O_2 \qquad (14)$$

By increasing the pH from 7 to 9, the removal efficiencies of COD (24.3%) and NH₃ (15.6%) slightly ascended. In alkaline medium, SO_5^{2-} was formed via the reaction between hydroxide and persulfate ions (Eq. 15). Afterwards, SO_5^{2} hydrolyzed to hydroperoxide anions (HO_2^-) in accordance with Eq. 16. Finally, the hydroperoxide anions became capable of activating persulfate in order to initiate sulfate radical formation (Eq. 17) (Furman et al., 2010; Liang & Guo, 2012).

$$S_2O_8^{2-} + OH^- \rightarrow HSO_4^- + SO_5^{2-} \qquad (15)$$

$$SO_5^{2-} + H_2O \rightarrow HO_2^- + SO_4^{2-} + H^+ \qquad (16)$$

$$S_2O_8^{2-} + HO_2^- \rightarrow SO_4^{2-} + SO_4^{\bullet-} + H^+ + O_2^{\bullet-} \qquad (17)$$
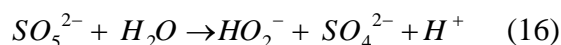
In the present study, a pH value, equal to 3 got selected for conducting the experiments. Fig. 6 shows the mechanism of pollutants

degradation by sulfate radical, produced through activation of PS by means of CS.

The removal tests of COD and NH_3 were carried out by means of PS, CS, and CS/PS processes. As shown in Fig. 7, in the PS process the removal efficiency of COD and NH_3 were 24.45% and 19.35%, respectively. On the other, the CS alone did not have any notable effect on removal ratios. The CS/PS process managed to increase the removal efficiency by more than 40%, compared to the PS process.

The ANOVA was utilized to estimate the models' validation along with variables' significance (Table 6). The model F- value of COD and NH_3 removal were (129.75) and (150.91), respectively.

The A, B, C, AB, AC, A^2, B^2, and C^2 were significant model terms for COD removal and the A, B, C, AB, AC, BC A^2, B^2, and C^2 for NH_3 removal, since terms with P-values below 0.05 were considered statistically significance (Silveira et al., 2017). Moreover, the slight difference between Pred R^2 and Adj R^2 indicated the models' accuracy. For the model to be eligible, its signal-to-noise ratio should stand above 4 (Prakash et al., 2013). In this study, these ratios for COD- and NH_3-removal models were 34.518 and 36.42, respectively. The p-values of lack of fit (LOF) for COD and NH_3 removal were not significant, due to the pure error, indicating that the model was prepared well.
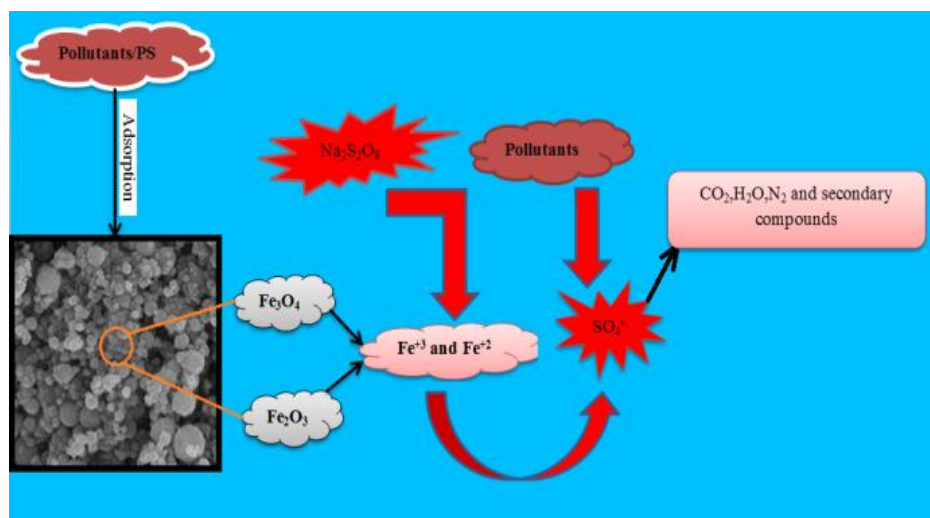
Fig. 6. Scheme 1. The suggested mechanism for pollutant degradation by CS activated persulfate
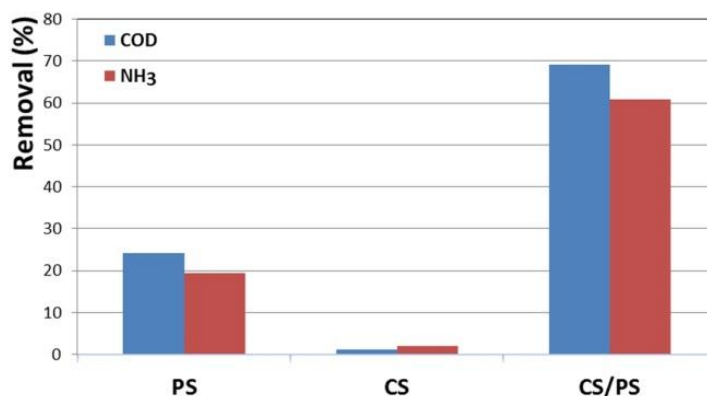
Fig. 7. Removal of COD and NH_3 in different systems; PS, CS, and CS/PS (PS/COD ratio:2; CS dose: 1.5 g L^{-1}; reaction time: 60 min ; pH 3.)

Table 6. ANOVA test for response function

	COD removal					NH$_3$ removal				
Source	**SS**	**Df**	**Mean square**	**F-value**	**p-value Probability > F**	**SS**	**Df**	**Mean square**	**F-value**	**p-value Probability > F**
Model	4132.20	9	459.13	129.75	< 0.0001	4487.86	9	498.65	150.91	< 0.0001
A(PS/COD)	1380.75	1	1380.75	390.21	< 0.0001	1280.18	1	1280.18	387.44	< 0.0001
B (CS)	1106.85	1	1106.85	312.80	< 0.0001	1297.95	1	1297.95	392.82	< 0.0001
C (PV)	800.00	1	800.00	226.08	< 0.0001	992.35	1	992.35	300.33	< 0.0001
AB	50.41	1	50.41	14.25	0.0069	48.30	1	48.30	14.62	0.0065
AC	49.70	1	49.70	14.05	0.0072	37.82	1	37.82	11.45	0.0117
BC	7.56	1	7.56	2.14	0.1872	64.00	1	64.00	19.37	0.0032
A^2	518.31	1	518.31	146.48	< 0.0001	489.30	1	489.30	148.08	< 0.0001
B^2	86.98	1	86.98	24.58	0.0016	114.07	1	114.07	34.52	0.0006
C^2	73.22	1	73.22	20.69	0.0026	97.21	1	97.21	29.42	0.0010
Residual	24.77	7	3.54			23.13	7	3.30		
Lack of Fit	12.48	3	4.16	1.35	0.3763	17.32	3	5.77	3.97	0.1080
Pure Error	12.29	4	3.07			5.81	4	1.45		
Cor total	4156.96	16				4510.99	16			
	Adj R^2= 0.9864, Pred R^2= 0.9474					Adj R^2= 0.9883, Pred R^2= 0.9366				

Based on the RSM model, the relation between COD and NH$_3$ removal, on one hand, and the operating parameters (PS/COD ratio, CS, and PV), on the other, were obtained in polynomial equations, in accordance with Eq. 18 and Eq. 19.

$$COD(\text{removal}\%)=-12.85+32.24A+12.91B$$
$$+0.62C+1.58AB-0.42AC+0.17BC \quad (18)$$
$$-4.93A^2-2.02B^2-0.137C^2$$

$$NH_3(\text{removal}\%)=-17.93+30.95A+13.04B$$
$$-0.24C+1.54AB-0.37AC+0.48BC \quad (19)$$
$$-4.79A^2-2.31B^2-0.159C^2$$

Where A is PS/COD ratio; B, CS (mg L^{-1}); and C, PV.

Figs. 8 (A to G) show 3D response surface of COD and NH$_3$ removal efficiency at center points with pH = 3. The Figs. 8 (A and E) show the relations of CS dose and PS/COD ratio at PV = 6.5 on COD and NH$_3$ removal efficiency, respectively. As noted in Figs. 8 (A and E), by increasing PS/COD ratio higher than the required limit, the efficiency of the removal rate remained stable. This can be explained by the fact that additional quantity of sulfate radicals was discouraged by interacting with one

another or with PS , based on Eq. 20 and Eq. 21 (Deng et al., 2013; Yang et al., 2011). It was also demonstrated that the excessive increase in CS dose did not lead to any significant change in removal effectiveness, since the saturation of the solution with iron ions can have a section of sulfate radicals destroyed, in accordance to Eq. 22 (Monteagudo et al., 2015; Yang et al., 2011).

$$SO_4^{\bullet-}+S_2O_8^{2-}\rightarrow S_2O_8^{-}+SO_4^{2-} \quad (20)$$

$$SO_4^{\bullet-}+SO_4^{\bullet-}\rightarrow S_2O_8^{2-} \quad (21)$$

$$Fe^{2+}+SO_4^{\bullet-}\rightarrow SO_4^{-}+Fe^{3+} \quad (22)$$
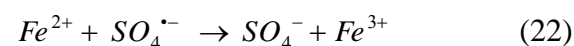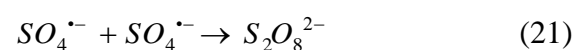
Fig. 8 (B and F) shows the relations of PV and PS/COD ratio at CS 2.5 g/L on COD and NH$_3$ removal efficiency, respectively. As can be seen in this figure, the removal efficiency of COD and NH$_3$ declined as the number of PV times rose. The main reason for that is the iron ions got solved in PRB only to come out with flowing leachate. The Fig. 8 (C and G) demonstrates the relations of PV and CS dose at PS/COD ratio 2 on COD and NH$_3$ removal efficiency, respectively, showing that by increasing CS dose, the number of PV, which could be treated, rose, which confirms the importance

of compensation for loss of CS in PRB by injecting the former into the latter. BBD was used to optimize the independent variables of COD and NH_3 removal. The PS/COD ratio: 3.47, CS: 3.09 g/L, and PV: 4.27 were the optimal operating conditions to achieve the minimizing operating costs with maximum

removal. In such conditions, the actual removal efficiency of COD and NH_3 were 74.2% and 66.8%, respectively, being within the 95%-prediction range. This confirms that the model's performance was good in terms of predicting the removal values.
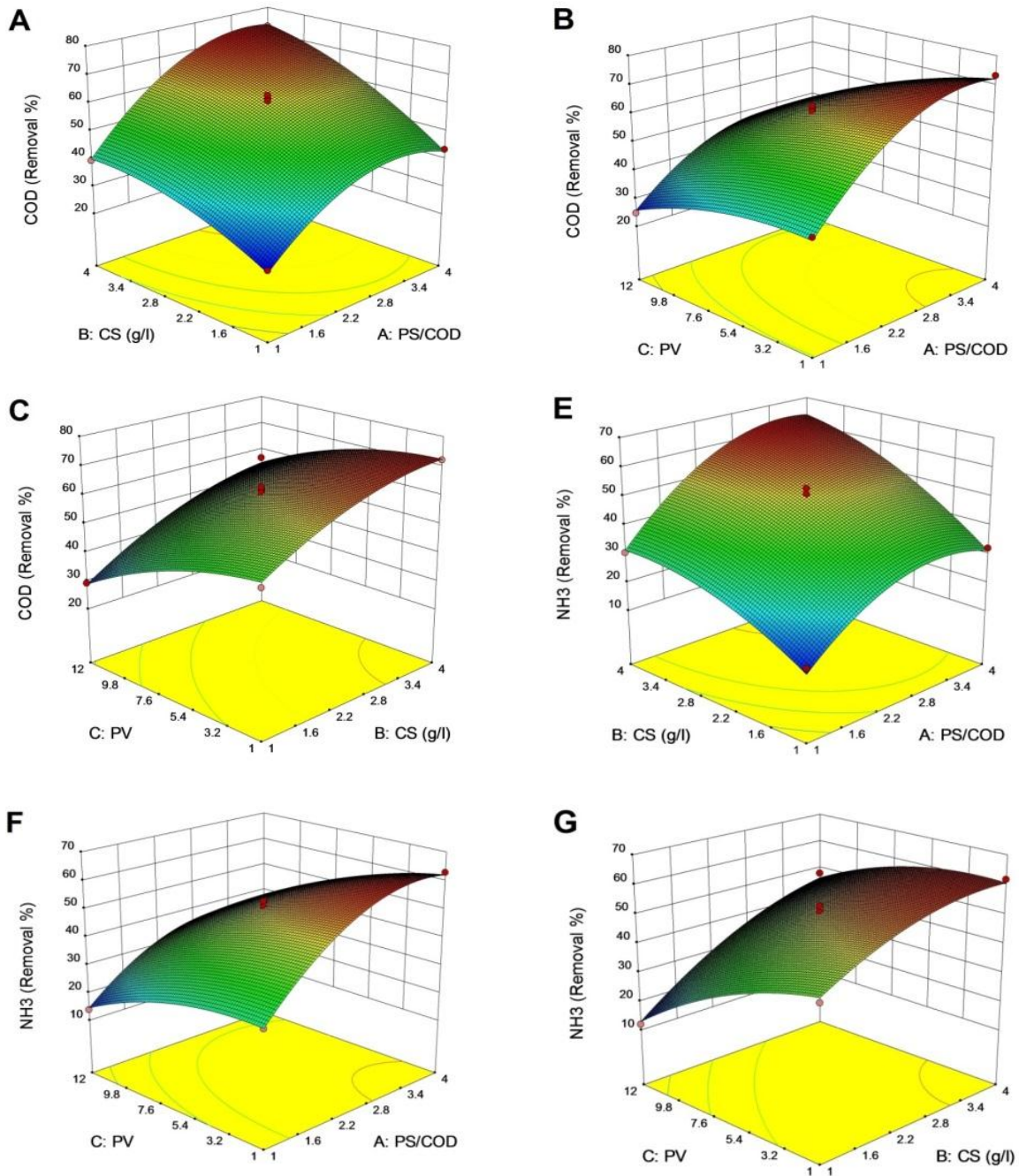
Fig. 8. 3D surface plot for COD and NH_3 removal efficiency at center points

Leachate landfill usually contains refractory-contaminated materials as well as persistent contaminated substances (Ranjbari & Mokhtarani, 2018). Several studies, using sulfate radical for treatment leachate landfill, have confirmed improvement of treated leachate's BOD_5/COD (Abu Amr et al., 2013; Hilles et al., 2016). The PS/CS process enhanced the BOD5/COD from 0.25 for raw leachate to 0.77 for treated leachate at the optimal operating conditions, as indicated in Fig. 9, which indicates that complex compounds were transformed into simpler ones. In order to ensure its validity, the SPE-GC-Mass spectrums for raw and treated leachate are displayed in Fig. 10 (A and B) and Table (7 and 8). The toxicity of the raw leachate was 0.263%, while after using PS/CS process, the toxicity dwindled to 0.0163% while the leachate landfill toxicity declined by more than 90%.
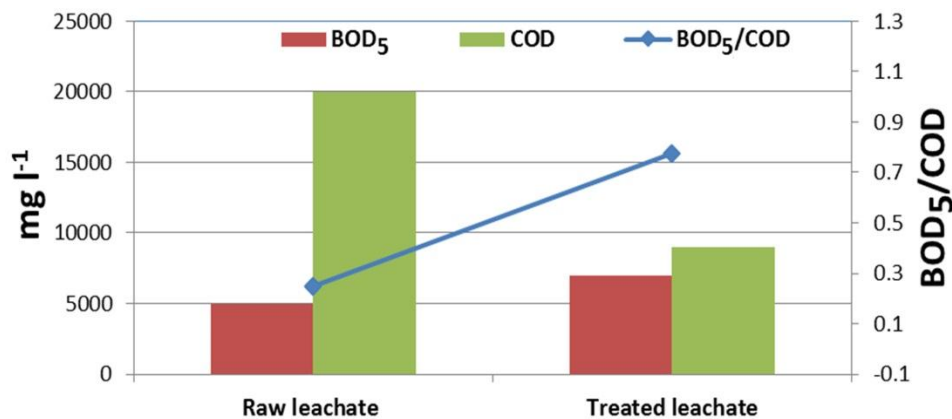
Fig. 9. Biodegradability of raw leachate and treated leachate
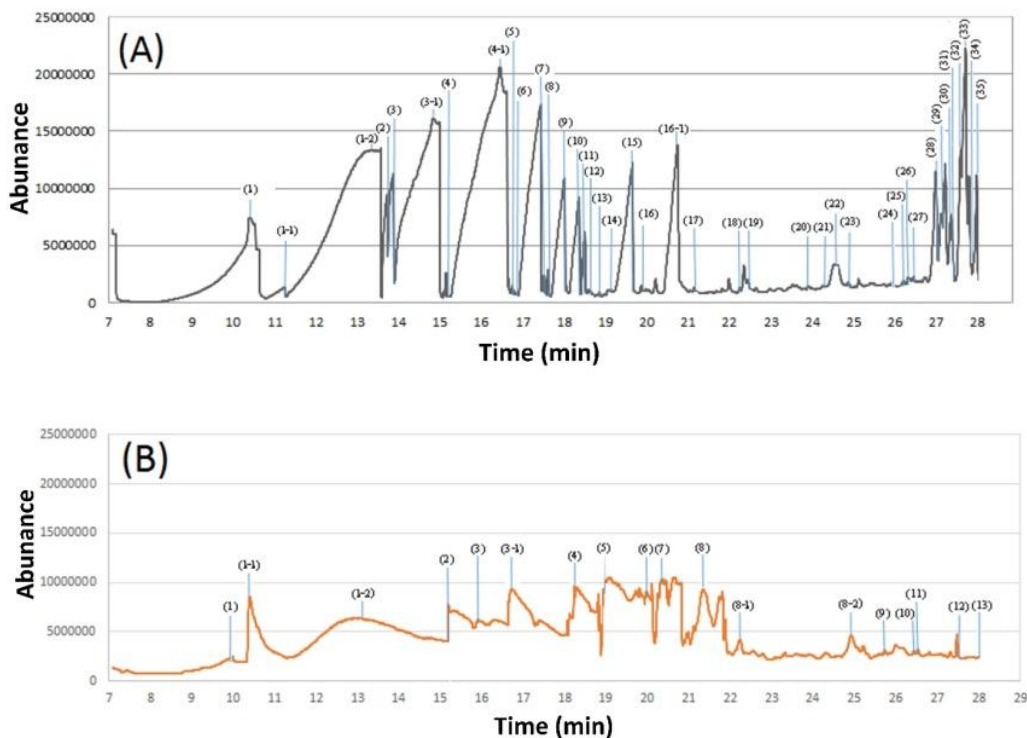
Fig. 10. GC-Mass spectra of the leachate: (a) raw and (b) treated leachate

Table 7. Raw leachate's identified constituents

Peak no	Compound	Retention time (min)	Fish LC50 (ppm)	Area%
1	Propanoic acid	10.39	248.12	13.9
1-1	Propanoic acid, 2-methyl-	11.25	294.06	0.53
1-2	Butanoic acid	13.57	139.34	35.26
2	Butanoic acid, 3-methyl-	13.73	159.31	1.32
3	Butanoic acid, 2-methyl-	13.87	182.16	1.9
3-1	Propanedioic acid, propyl-	18.84	120.70	31.14
4	Pentanoic acid, 4-methyl	15.15	110.13	1.05
4-1	Hexanoic acid	16.45	56.57	36.45
5	5-METHYLHEXANOIC	16.76	22.75	0.3
6	Hexanoic acid, 4-methyl-	16.81	53.71	0.15
7	Propanoic acid, 3-(methylthio)-	17.51	169.01	0.6
8	Hexanoic acid, 2-ethyl-	17.61	27.76	0.9
9	Cyclohexanecarboxylic acid	18.01	53.73	5.32
10	Octanoic acid	18.37	9.04	16.2
11	Benzoic acid	18.50	106.35	1.02
12	Butanoic acid, 4-(methylthio)-	18.6	124.53	0.45
13	Octanoic acid	18.86	9.04	0.3
14	2-Piperidinone	19.06	473.88	0.15
15	Benzeneacetic acid	19.65	70.16	6.66
16	Caprolactam	19.86	329.35	0.35
16-1	Benzenepropanoic acid	20.74	61.13	7.21
17	2H-1-Benzopyran-2-one	21.14	87.84	0.3
18	Bicyclo[3.1.1]heptane, 2,6,6- trimethyl -	22.25	0.93	0.2
19	2H-Indol-2-one, 1,3-dihydro-	22.45	101.09	0.3
20	Ibuprofen	23.90	2.55	0.4
21	7-Pentadecyne	24.25	0.58	0.2
22	Acetic acid, phenoxy-, methyl ester	24.53	20.09	1.15
23	2,2-Dimethyl-5-hydroxy-7-methoxy-chromanone	24.87	8.96	0.3
24	Cyclopentadecanone, 2-hydroxy-	25.85	137	0.1
25	11-Dodecenyl trifluoroacetate	26.20	1.72	0.4
26	6(E),8(E)-Heptadecadiene	26.33	0.21	0.5
27	1,2-Benzenedicarboxylic acid, bis(2-methylpropyl) ester	26.45	4.16	0.2
28	1,2-Benzenedicarboxylic acid, diisooctyl ester	26.98	1.82	0.3
29	Di-(2-ethylhexyl)phthalate	27.12	0.33	2.2
30	Di-(2-ethylhexyl)phthalate	27.22	0.33	5.05
31	Di-(2-ethylhexyl)phthalate	27.36	0.33	5.7
32	1,2-Benzenedicarboxylic acid, diisooctyl ester	27.59	1.82	3.6
33	1,2-Benzenedicarboxylic acid, diisooctyl ester	27.71	1.82	2.98
34	Di-(2-ethylhexyl)phthalate	27.79	0.33	2.95
35	Di-(2-ethylhexyl)phthalate	27.97	0.33	7.1

Table 8. Treated leachate's identified constituents

Peak no	Compound	Retention time (min)	Fish LC50 (ppm)	Area%
1	Propanoic acid	9.98	248.12	2.04
1-1	Tetrachloroethylene	10.40	15.65	25.9
1-2	Butanoic acid	12.95	139.34	15.21
2	Butanoic acid, 3-methyl-	15.20	159.31	2.12
3	Pentanoic acid	15.9	299.91	1.33
3-1	Hexanoic acid	16.73	56.57	3.12
4	Hexanoic acid, 2-ethyl-	18.85	27.76	2.74
5	Cyclohexanecarboxylic acid	18.98	53.73	3.3
6	Benzoic Acid	19.97	106.35	1.01
7	Heptanoic acid	20.37	22.75	13.85
8	1-Cyclohexene-1-carboxylic acid	21.36	27.54	12.18
8-1	8-Chlorocapric acid	22.23	6.98	2.34
8-2	Azelaic acid	24.92	13.22	4.72
9	Oleyl Alcohol	25.73	0.8	0.27
10	9-Octadecenoic acid, (E)-	26.44	0.22	0.26
11	Diethyl Phthalate	26.53	3.52	0.3
12	Dibutyl phthalate	27.48	1.11	1.43
13	Citronellal	27.98	2.72	0.12

CONCLUSION

The study investigated the possibility of using CS as a wastage-material for activating PS oxidation in PRB technology. Experiments showed that CS could be considered a good source of iron ions. The XRD analysis confirmed the presence of iron oxides, with EDS analysis showing an iron component with a ratio of up to more than 70%. BBD was used to optimize the independent variables of COD and NH_3 removal from leachate landfill. The PS/COD ratio: 3.47, CS: 3.09 g/L, and PV: 4.27 were the optimal operating conditions to achieve minimum operating costs with maximum removal. SPE-GC-MS analysis indicated that during the integrated process, most of the refractory-contaminated materials can be transformed into simpler compounds.

ACKNOWLEDGMENTS

REFERENCES

Abbas, A. A., Jingsong, G., Ping, L. Z., Ya, P. Y. and Al-Rekabi, W. S. (2009). Review on landfill leachate treatments. *American Journal of Applied Sciences.*, 6(4); 672–684.

Abhayawardana, G. P. R. (2015). Removal of Lead in Landfill Leachate using Permeable Reactive Barriers with Natural Red Earth and Peat. The Institution of Engineers, Sri Lan., XLVIII(4); 51–57.

Abu Amr, S. S., Aziz, H. A., Adlan, M. N. and Bashir, M. J. K. (2013). Pretreatment of stabilized leachate using ozone/persulfate oxidation process. *Chemical Engineering Journal.*, 221; 492–499

Ahmad, A., Gu, X., Li, L., Lv, S., Xu, Y. and Guo, X. (2015). Efficient degradation of trichloroethylene in water using persulfate activated by reduced graphene oxide-iron nanocomposite. *Environmental Science and Pollution Research.*, 22(22); 17876–17885.

Al-Shamsi, M. A. and Thomson, N. R. (2013). Treatment of a trichloroethylene source zone using persulfate activated by an emplaced nano-Pd-Fe0zone. *Water, Air, and Soil Pollution.*, 224(11);1-12.

Bartzas, G., Komnitsas, K. and Paspaliaris, I. (2006). Laboratory evaluation of Fe0 barriers to treat acidic leachates. *Minerals Engineering.*, 19(5); 505–514.

Bhalla, B., Saini, M. S., Jha, M. K., Scientist, C., Gujral, P. and City, S. (2014). Assessment of industrial byproducts as permeable reactive barriers for landfill leachate Management. International Journal of Research in Engineering and Technology., 3(3); 637–648.

Bozkurt, M. A., Akdeniz, H., Keskin, B. and Yilmaz, I. H. (2006). Possibilities of using sewage sludge as nitrogen fertilizer for maize. *Acta Agriculturae Scandinavica Section B-Soil and Plant Science.*, 56(2); 143–149.

Cao, J., Zhang, W.-X., Brown, D. G. and Sethi, D. (2008). Oxidation of Lindane with Fe(II)-Activated Sodium Persulfate. *Environmental Engineering Science.*, 25(2); 221–228.

Chiemchaisri, C., Chiemchaisri, W. and Witthayapirom, C. (2015). Remediation of MSW landfill leachate by permeable reactive barrier with vegetation. *Water Science and Technology.*, 71(9); 1389–1397.

Chou, Y. C., Lo, S. L., Kuo, J. and Yeh, C. J. (2013). Derivative mechanisms of organic acids in microwave oxidation of landfill leachate. *Journal of Hazardous Materials.*, 254–255(1); 293–300.

Chung, H. I., Kim, S. K., Lee, Y. S. and Yu, J. (2007). Permeable reactive barrier using atomized slag material for treatment of contaminants from landfills. *Geosciences Journal.*, 11(2); 137–145.

Czurda, K. A. and Haus, R. (2002). Reactive barriers with fly ash zeolites for in situ groundwater remediation. *Applied Clay Science.*, 21(2); 13–20.

Daoud, W., Ebadi, T. and Fahimifar, A. (2015). Removal of hexavalent chromium from aqueous solutions using micro zero-valent iron supported by bentonite layer. *Water Science and Technology.*, 71(5); 667–674.

Deng, J., Shao, Y., Gao, N., Deng, Y., Tan, C. and Zhou, S. (2013). Zero-valent iron/persulfate(Fe0/PS) oxidation acetaminophen in water. *International Journal of Environmental Science and Technology.*, 11(4; 881–890.

Deng, Y. and Ezyske, C. M. (2011). Sulfate radical-advanced oxidation process (SR-AOP) for simultaneous removal of refractory organic contaminants and ammonia in landfill leachate. *Water Research.*, 45(18); 6189–6194.

Devi, L. G., Kumar, S. G., Raju, K. S. A. and Rajashekhar, K. E. (2010). Photo-Fenton and photo-Fenton-like processes for the degradation of methyl orange in aqueous medium : Influence of oxidation states of iron., 64(3); 378–385.

Diao, Z., Xu, X., Chen, H., Jiang, D., Yang, Y., Kong, L. and Liu, L. (2016). Simultaneous removal of Cr (VI) and phenol by persulfate activated with bentonite-supported nanoscale zero-valent iron : Reactivity and mechanism. *Journal of Hazardous Materials.*, *316*; 186–193.

Fang, G., Dionysiou, D. D., Al-abed, S. R. and Zhou, D. (2013). Applied Catalysis B : Environmental Superoxide radical driving the activation of persulfate by magnetite nanoparticles : Implications for the degradation of PCBs. *Applied Catalysis B, Environmental.*, *129;* 325–332.

Furman, O. S., Teel, A. M. Y. L. and Watts, R. J. (2010). Mechanism of Base Activation of Persulfate., (509); 6423–6428.

Govindan, K., Raja, M., Maheshwari, S. U. and Noel, M. (2014). Analysis and understanding of amido black 10B dye degradation in aqueous solution by electrocoagulation with the conventional oxidants peroxomonosulfate, peroxodisulfate and hydrogen peroxide. *Environ. Sci.: Water Res. Technol.*, *1*(1); 108–119.

Hilles, A. H., Abu Amr, S. S., Hussein, R. A., El-Sebaie, O. D. and Arafa, A. I. (2016). Performance of combined sodium persulfate/H_2O_2 based advanced oxidation process in stabilized landfill leachate treatment. *Journal of Environmental Management.*, *166*; 493–498.

Hou, L., Zhang, H. and Xue, X. (2012). Ultrasound enhanced heterogeneous activation of peroxydisulfate by bimetallic Fe-Co/GAC catalyst for the degradation of Acid Orange 7 in water. *Journal of Environmental Sciences (China).*, *26*(6); 1267–1273.

House, D. A. (1962). Kinetics and Mechanism of Oxidations by Peroxydisulfate. *Chemical Reviews.*, *62*(3); 185–203.

Huling, S. G., Ko, S., Park, S. and Kan, E. (2011). Persulfate oxidation of MTBE- and chloroform-spent granular activated carbon ૯. *Journal of Hazardous Materials.*, *192*(3); 1484–1490.

Huling, S. G. and Pivetz, B. E. (2006). Engineering issue paper: in-situ chemical oxidation. *Washington: U.S. EPA.*, 2006.

Joanna, F. and Kazimierz, G. (2013). Evaluation of zeolite-sand mixtures as reactive materials protecting groundwater at waste disposal sites. *Journal of Environmental Sciences (China).*, *25*(9); 1764–1772.

Jun, D., Yongsheng, Z., Weihong, Z. and Mei, H. (2009). Laboratory study on sequenced permeable reactive barrier remediation for landfill leachate-contaminated groundwater. *Journal of Hazardous Materials.*, *161*(1); 224–230.

Karchegani, S. M., Hoodaji, M. and Kalbasi, M. (2014). The effect of steel converter slag application along with sewage sludge in iron nutrition and corn plant yield., *3*(Iii); 96–104.

Karimian, N., Kalbasi, M. and Hajrasuliha, S. (2012). Effect of converter sludge , and its mixtures with organic matter , elemental sulfur and sulfuric acid on availability of iron , phosphorus and manganese of 3 calcareous soils from central Iran., *7*(4); 568–576.

Kolthoff, I. M. and Miller, I. K. (1951). The Chemistry of Persulfate. I. The Kinetics and Mechanism of the Decomposition of the Persulfate Ion in Aqueous Medium1, *899*(6).

Kumar, A., Prasad, B. and Mishra, I. M. (2008). Optimization of process parameters for acrylonitrile removal by a low-cost adsorbent using Box-Behnken design. *Journal of Hazardous Materials.*, *150*(1); 174–182.

Oh, B. T., Lee, J. Y. and Yoon, J. (2007). Removal of contaminants in leachate from landfill by waste steel scrap and converter slag. Environ Geochem Health., 29; 331–336.

Liang, C., Bruell, C. J., Marley, M. C.and Sperry, K. L. (2004). Persulfate oxidation for in situ remediation of TCE. I. Activated by ferrous ion with and without a persulfate-thiosulfate redox couple. *Chemosphere.*, *55*(9); 1213–1223.

Liang, C. and Guo, Y. Y. (2012). Remediation of diesel-contaminated soils using persulfate under alkaline condition. *Water, Air, and Soil Pollution.*, *223*(7); 4605–4614.

Liang, C., Wang, Z. S. and Bruell, C. J. (2007). Influence of pH on persulfate oxidation of TCE at ambient temperatures. *Chemosphere.*, *66*(1); 106–113.

Lin, Y. T., Liang, C. and Chen, J. H. (2011). Feasibility study of ultraviolet activated persulfate oxidation of phenol. *Chemosphere.*, *82*(8); 1168–1172.

Liu, D., Xiu, Z., Liu, F., Wu, G., Adamson, D., Newell, C., … Alvarez, P. J. (2013). Perfluorooctanoic acid degradation in the presence of Fe(III) under natural sunlight. *Journal of Hazardous Materials.*, *262*; 456–463.

Liu, J., Zeng, N. and Xu, W. (2011). Effects of the Use of Permeable Barrier for Landfill Leachate Treatment. *Journal of Water and Environment Technology.*, *9*(2); 209–214.

Madani, K., AghaKouchak, A. and Mirchi, A. (2016). Iran's Socio-economic Drought: Challenges of a Water-Bankrupt Nation. *Iranian Studies.*, *49*(6); 997–1016.

Mokhtarani, N., Khodabakhshi, S. and Ayati, B. (2016). Optimization of photocatalytic post-treatment of composting leachate using UV/TiO2. *Desalination and Water Treatment.*, *57*(47); 22232–22243.

Monteagudo, J. M., Durán, A., González, R. and Expósito, A. J. (2015). In situ chemical oxidation of carbamazepine solutions using persulfate simultaneously activated by heat energy, UV light, Fe^{2+} ions, and H_2O_2. *Applied Catalysis B: Environmental.*, *176–177*; 120–129.

Nachiappan, S. and Gopinath, K. P. (2015). Treatment of pharmaceutical effluent using novel heterogeneous fly ash activated persulfate system. *Journal of Environmental Chemical Engineering.*, *3*(3); 2229–2235.

NRC. (1999). Groundwater and Soil Cleanup: Improving Management of Persistent Contaminants. *Washington: National Academy Press*, 1999.

Ortiz, N., Pires, M. A. F. and Bressiani, J. C. (2001). Use of steel converter slag as nickel adsorber to wastewater treatment. *Waste Management. ,21*; 631–635.

Pazoki, M., Abdoli, M. A., Karbassi, A., Mehrdadi, N. and Yaghmaeian, K. (2014). Attenuation of municipal landfill leachate through land treatment. *International Journal of Environmental Health Science & Engineering.*, *1*(12); 1–8.

Prakash .M, J., Manikandan, S., Thirugnanasambandham, K., Vigna Nivetha, C. and Dinesh, R. (2013). Box-Behnken design based statistical modeling for ultrasound-assisted extraction of corn silk polysaccharide. *Carbohydrate Polymers.*, *92*(1); 604–611.

Ranjbari, A. and Mokhtarani, N. (2018). Post treatment of composting leachate using ZnO nanoparticles immobilized on moving media. *Applied Catalysis B: Environmental.*, *220*; 211–221.

Renou, S., Givaudan, J. G., Poulain, S., Dirassouyan, F. and Moulin, P. (2008). Landfill leachate treatment: Review and opportunity. *Journal of Hazardous Materials.*, *150*(3); 468–493.

Romero, A., Santos, A., Vicente, F. and González, C. (2010). Diuron abatement using activated persulphate: Effect of pH, Fe(II) and oxidant dosage. *Chemical Engineering Journal.*, *162*(1); 257–265.

Shiying, Y., Wang, P., Yang, X., Wei, G., Zhang, W. and Shan, L. (2009). A novel advanced oxidation process to degrade organic pollutants in wastewater: Microwave-activated persulfate oxidation. *Journal of Environmental Sciences.*, *21*(9); 1175–1180.

Siegrist, R. L., Crimi, M. and Simpkin, T. J. (2011). In situ chemicaloxidation for groundwater remediation. *NewYork: Springer.*, 2011.

Silveira, J. E., Barreto-Rodrigues, M., Cardoso, T. O., Pliego, G., Munoz, M., Zazo, J. A. and Casas, J. A. (2017). Nanoscale Fe/Ag particles activated persulfate: Optimization using response surface methodology. *Water Science and Technology.*, *75*(9); 2216–2224.

Soubh, A. M., Baghdadi, M., Abdoli, M. A. and Aminzadeh, B. (2018). Activation of Persulfate Using an Industrial Iron-Rich Sludge as an Efficient Nanocatalyst for Landfill. *Catalysts.*, *8*(5); 218.

Soubh, A. and Mokhtarani, N. (2016). The post treatment of composting leachate with a combination of ozone and persulfate oxidation processes. *Rsc Adv*ances, *6*(80); 76113–76122.

Van-Nooten, T., Diels, L. and Bastiaens, L. (2010). Design of a multibarrier for the treatment of landfill leachate contamination: laboratory column evaluation. *4th International Symposium: Permeable Reactive Barriers and Reactive Zones.*, *42*(23); 34.

Virtanen, S., Schmuki, P., Davenport, A. J. and Vitus, C. M. (1997). Dissolution of Thin Iron Oxide Films Used as Models for Iron Passive Films Studied by In Situ X-Ray Absorption Near-Edge Spectroscopy. *Journal of The Electrochemical Society.*, *144*(1); 198.

Yan, J., Lei, M., Zhu, L., Anjum, M. N., Zou, J. and Tang, H. (2011). Degradation of sulfamonomethoxine with Fe3O4 magnetic nanoparticles as heterogeneous activator of persulfate. *Journal of Hazardous Materials.*, *186*(2–3); 1398–1404.

Yang, S., Yang, X., Shao, X., Niu, R. and Wang, L. (2011). Activated carbon catalyzed persulfate oxidation of Azo dye acid orange 7 at ambient temperature. *Journal of Hazardous Materials.*, *186*(1); 659–666.

Zhen, G., Lu, X., Zhao, Y., Chai, X. and Niu, D. (2012). Enhanced dewaterability of sewage sludge in the presence of Fe(II)-activated persulfate oxidation. *Bioresource Technology.*, *116*; 259–265.